Characteristics of ultrashallow p^+/n junction prepared cluster boron ($B_{18}H_{22}$) ion implantation and excimer laser annealing

Sungho Heo, Seokjoon Oh, Musarrat Hasan, H.T. Cho[1], W.A. Krull[1], and Hyunsang Hwang*

Gwang-Ju Institute of Science and Technology (GIST)
Department of Materials Science and Engineering, #1, Oryong-Dong, Buk-Gu, Gwang-Ju, 500-712, Korea
[1] SemEquip, Inc, 34 Sullivan Road, Billerica, Massachusetts, USA, 01862
Tel: (+82 62) 970-2314, Fax: (+82 62) 970-2304, *E-mail: hwanghs@gist.ac.kr

Abstract

Ultrashallow junction (<10nm) p^+/n junction formed by $B_{18}H_{22}$ cluster ion implantation and excimer laser annealing (ELA) is demonstrated. $B_{18}H_{22}^+$ equivalent implantation energy at 0.25 keV readily forms an amorphous-silicon (a-Si) layer without additional Si^+ or Ge^+ implantation. After ELA at 500 mJ/cm^2, diffusion of the boron profile was almost negligible, which can be explained by selective melting of a-Si.

1. Introduction

Conventional B^+ and BF_2^+ implantation generally cannot satisfy the requirement of p^+/n junction depth for sub-45 CMOS devices. Ultra-low energy B^+ implantation exhibits very low throughput due to low beam current (current α energy$^{3/2}$). For BF_2^+ implantation, the dopant activation rate normally degrades due to the presence of fluorine. $B_{18}H_{22}^+$ can effectively make an a-Si layer without additional Si^+ or Ge^+ implantation and reduce boron channeling due to its 20 times higher mass than relative to boron. It has various advantages such as high throughput, low beam divergence, and high dose implantation. However, B^+ like implantation, cluster boron ion implantation also shows transient enhance diffusion (TED) during rapid thermal annealing (RTA), which increases the junction depth.[1] To solve this problem, we applied ELA of $B_{18}H_{22}^+$ implanted samples. In addition, we studied on $B_{18}H_{22}^+$ implantation issues such as incorporated hydrogen and surface morphology.

2. Experimental

$B_{18}H_{22}$ cluster ions at an equivalent energy of 0.25 ~ 1 keV were implanted to an actual dose of $3 \times 10^{14} \sim 1 \times 10^{15}$ /cm^2 into n-type Si substrates. ELA was conducted with an energy of 300 ~ 700 mJ/cm^2 at 1 pulse in the p^+/n junction. The sheet resistance (R_s) and active carrier concentration (N_s) were measured by Hall measurement. Atomic force microscopy (AFM) and high-resolution cross-sectional transmission electron microscopy (HR-XTEM) analysis were conducted. The boron dopant depth profiles were obtained by secondary ion mass spectrometry (SIMS).

3. Results and discussion

Up to 500mJ/cm^2, the R_s decreased below 830 ohm/sq. and the dopant activation rate was increased above 72% as shown in Fig. 1. This indicates that laser energy above 500 mJ/cm^2 is sufficient for dopant activation, perhaps owing to re-crystallization of the melted a-Si layer as shown in Fig. 2.(a),(b). The a-Si melting temperature is normally 300 ^{o}C lower than crystalline-Si (c-Si) layer. The proposed approach of $B_{18}H_{22}^+$ ion implantation with ELA at 500 mJ/cm^2 is expected to mitigate the problem of process integration.

The critical ELA energy is directly related to the a-Si thickness and implanted dose for dopant activation. Compared with RTA, ELA shows improved R_s and N_s results as shown in Fig. 3, which are attributed to dopant activation above the solid solubility limit. The sample implanted at energy of 1keV shows lower R_s and higher N_s values after ELA than that of the control sample implanted at 0.25keV, which can be explained by the deeper junction depth. The high dose implanted sample shows a lower R_s value than that of the control sample without any increase in the implantation energy due to the increase of dopant activation.

Figure 4 shows the boron SIMS depth profile after various process conditions. For comparison, the as-implanted monomer ^{11}B profile was calculated by Monte Carlo simulations. Compared with the simulated monomer ^{11}B depth profile, the $B_{18}H_{22}^+$ implanted sample shows a dramatic reduction of the boron channeling tail and improved vertical abruptness. After ELA at 500 mJ/cm^2, diffusion of the boron profile was almost negligible, which can be explained by selective melting of a-Si.

Hydrogen is co-implanted during the $B_{18}H_{22}^+$ implantation. However, this hydrogen only affects near surface region as shown in Fig. 5. The reason is that incorporated hydrogen has a small fractional of total equivalent energy. After ELA, almost all hydrogen diffuses out similar as RTA at 500℃. Therefore, $B_{18}H_{22}^+$ implantation with ELA may not consider the influence of incorporated hydrogen.

Compared with monomer $^{11}B^+$ implantation, $B_{18}H_{22}^+$ implantation has a different damage and surface morphology. Hence, we conducted AFM analysis as shown in Fig. 6. $B_{18}H_{22}^+$ as-implanted sample shows low RMS value. After ELA at 500mJ/cm^2, the change of RMS value was negligible due to low laser energy.

Figure 7 shows the relationship of R_s and X_j obtained in this experiment as well as reported results.[2] Implantation of various dopants such as B^+, BF_2^+, $B_{10}H_{14}^+$, and $B_{18}H_{22}^+$ and various annealing methods were evaluated. Compared with the reported results, our samples show shallower X_j and lower R_s.

4. Conclusions

In summary, a sub-10nm ultrashallow p^+/n junction formed by $B_{18}H_{22}$ cluster ion implantation and ELA is demonstrated. The ELA yielded shallow X_j (~ 9nm) and low R_s (~830ohm/sq.), which are attributed to reduced TED. Considering the various advantages noted here, the $B_{18}H_{22}^+$ implantation with ELA appears to be a promising process for the sub-45nm CMOS technology node.

1-4244-0047-3/06/$20.00 ©2006 IEEE.

Acknowledgements

The authors would like to thank J. W. Marino in Charles Evans Association for providing SIMS analysis.

References

[1] A. Agawal, H.-J. Gossmann, D. C. Jacobson, D. J. Eaglesham, M. Sosnowski, J. M. Poate, I. Yamada, J. Matsuo, and T. E. Haynes, Appl. Phys. Lett. **73**, (1998) 2015.

[2] K. Suguro, T. Ito, K. Matsuo, T. Iinuma, and K. T. Nishinohara, *Ext. Abs. of the 4th inter. Workshop on Junction Technol.*(Shanghai, china, 2004) p. 18.

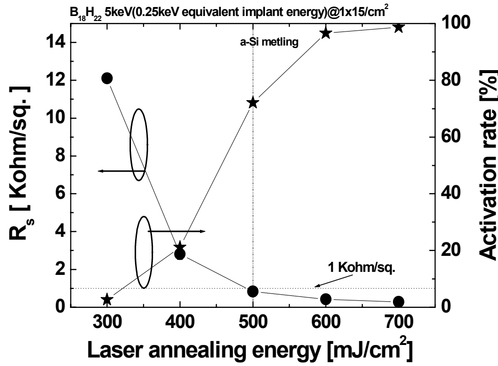

Fig. 1 Variation of sheet resistance (R_s) and activation rate (%) as a function of ELA energy of 300 ~ 700 mJ/cm^2.

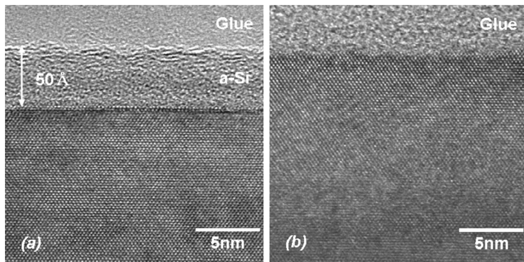

Fig. 2 The X-TEM images of (a) the as-implanted sample of equivalent energy at 0.25 keV and (b) ELA at 500 mJ/cm^2.

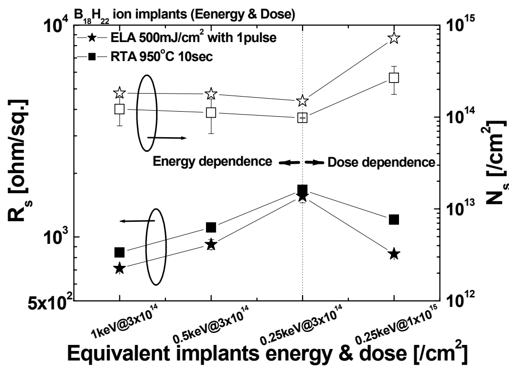

Fig. 3 Variation of R_s and N_s as a function of implanted conditions (energy & dose) with annealing methods.

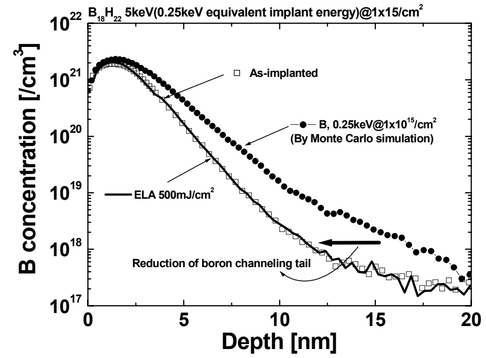

Fig. 4 SIMS depth profile of boron before and after ELA. The as-implanted monomer ^{11}B profile was calculated by Monte Carlo simulations.

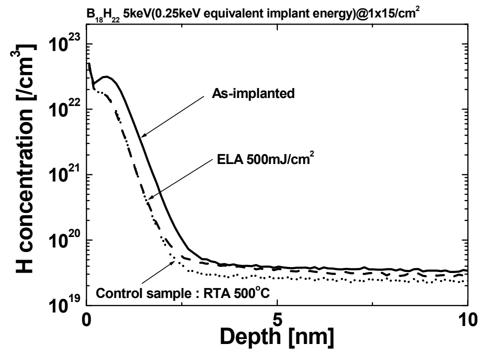

Fig. 5 SIMS depth profile of hydrogen before and after ELA Control sample shows hydrogen profile after RTA at 500℃.

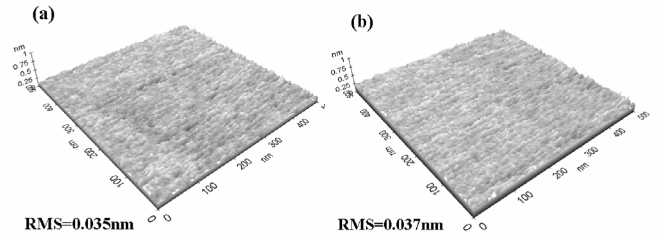

Fig. 6 Three-dimensional (3D) AFM images and RMS values of (a) the as-implanted sample of equivalent energy at 0.25 keV and (b) ELA at 500 mJ/cm^2.

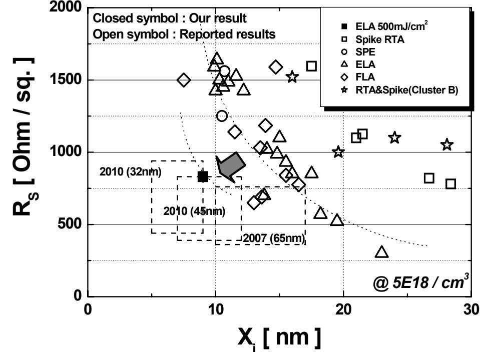

Fig. 7 Relationship of R_s vs. X_j. The closed and open symbols denote this experiment and reported results, respectively.